Dynamical Creation of a Supersolid in Asymmetric Mixtures of Bosons

Tassilo Keilmann,[1] Ignacio Cirac,[1] and Tommaso Roscilde[1,2]

[1]*Max-Planck-Institut für Quantenoptik, Hans-Kopfermann-Strasse 1, Garching, D-85748, Germany*

[2]*Ecole Normale Supérieure, 46 Allée d'Italie, F-69007 Lyon, France*

(Received 19 May 2009; published 26 June 2009)

We propose a scheme to dynamically create a supersolid state in an optical lattice, using an attractive mixture of mass-imbalanced bosons. Starting from a "molecular" quantum crystal, supersolidity is induced dynamically as an out-of-equilibrium state. When neighboring molecular wave functions overlap, both bosonic species simultaneously exhibit quasicondensation and long-range solid order, which is stabilized by their mass imbalance. Supersolidity appears in a perfect one-dimensional crystal, without the requirement of doping. Our model can be realized in present experiments with bosonic mixtures that feature simple on-site interactions, clearing the path to the observation of supersolidity.

DOI: 10.1103/PhysRevLett.102.255304 PACS numbers: 67.80.kb, 05.30.Jp, 37.10.Jk, 67.60.Bc

The intriguing possibility of creating a quantum hybrid exhibiting both superflow and solidity was envisioned long ago [1]. However, its experimental observation remains elusive. The quest for supersolidity has been strongly revitalized by recent experiments showing possible evidence for a nonzero superfluid fraction present in solid ^{4}He [2]. Yet, several theoretical results [3] appear to rule out the presence of condensation in the pure solid phase of ^{4}He, and various experiments [4] show indeed a strong dependence of the superfluid fraction on extrinsic effects, such as ^{3}He impurities and dislocations. While the experimental findings on bulk ^{4}He remain controversial, optical-lattice setups [5] offer the advantages of high sample purity and experimental control to directly pin down a supersolid state via standard measurement techniques. A variety of lattice-boson models with strong finite-range interactions have been recently shown to display crystalline order and supersolidity upon doping the crystal state away from commensurate filling [3,6]; yet sizable interactions with a finite range are generally not available in current cold-atom experiments. Such interactions can be, in principle, obtained effectively by adding a second atomic species of fermions [7], which, however, does not participate in the condensate state, in a way similar to the nuclei forming the lattice of a superconductor without participating in the condensate of electron pairs.

Here we demonstrate theoretically a new route to supersolidity, realized as the out-of-equilibrium state of a realistic lattice-boson model after a so-called "quantum quench" (a sudden change in the Hamiltonian). The equilibrium Hamiltonian of the model before the quench realizes a "molecular crystal" phase characterized by the crystallization of atomic trimers made of two mass-imbalanced bosonic species. Starting from a solid of tightly bound trimers and suddenly changing the system Hamiltonian, the evolution induces broadening and overlap of neighboring molecular wave functions leading to quasicondensation of all atomic species, while crystalline order is maintained (Fig. 1). Our model requires only local on-site interactions as currently featured by neutral cold atoms, which make the observation of a supersolid state a realistic and viable goal.

We consider two bosonic species ($\sigma = \uparrow, \downarrow$) tightly confined in two transverse spatial dimensions and loaded in an

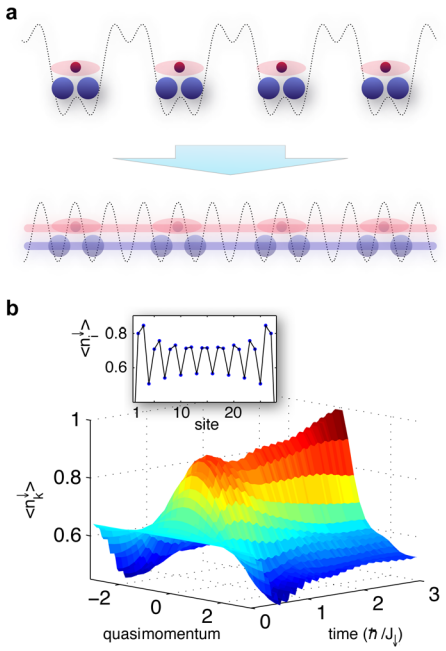

FIG. 1 (color online). Dynamical onset of supersolidity by quantum quenching a mixture of light and heavy bosons. (a) A product state of bosonic trimers is the initial state of the evolution (larger symbols represent the ↓ bosons); switching off one of the superlattice components leads to a supersolid state in which the particles delocalize into a (quasi)condensate while maintaining the original solid pattern without imperfections. (b) Momentum profile of the ↓ bosons, $\langle n_k^\downarrow \rangle$ versus time in units of hopping events $\hbar/J_\downarrow$. A quasicondensate peak develops rapidly. Inset: Density distribution $\langle n_i^\downarrow \rangle$ averaged over the last third of the evolution time, showing that crystalline order is conserved in the system. (The simulation parameters are $L = 28$, $N_\downarrow = 18$, $N_\uparrow = 9$, $J_\downarrow/J_\uparrow = 0.1$, $U/J_\uparrow = 3.0$.)

optical-lattice potential in the third dimension. In the limit of a deep optical lattice, the dynamics of the atoms can be described by a model of lattice hard-core bosons in one dimension [8,9],

$$\mathcal{H} = -\sum_{i,\sigma} J_\sigma (b^\dagger_{i,\sigma} b_{i+1,\sigma} + \text{H.c.}) - U \sum_i n_{i,\uparrow} n_{i,\downarrow}. \quad (1)$$

Here the operator $b^\dagger_{i\sigma}$ ($b_{i\sigma}$) creates (annihilates) a hard-core boson of species σ on site i of a chain of length L, and it obeys the on-site anticommutation relations $\{b_{i\sigma}, b^\dagger_{i\sigma}\} = 1$. $n_{i\sigma} \equiv b^\dagger_{i\sigma} b_{i\sigma}$ is the number operator. Throughout this Letter we restrict ourselves to the case of attractive on-site interactions $U > 0$ and to the case of mass imbalance $J_\uparrow > J_\downarrow$. Moreover we fix the lattice fillings of the two species to $n_\uparrow = 1/3$ and $n_\downarrow = 2/3$.

In the extreme limit of mass imbalance $J_\downarrow = 0$, Eq. (1) reduces to the well-known Falicov-Kimball model of mobile particles in a potential created by static impurities [10].

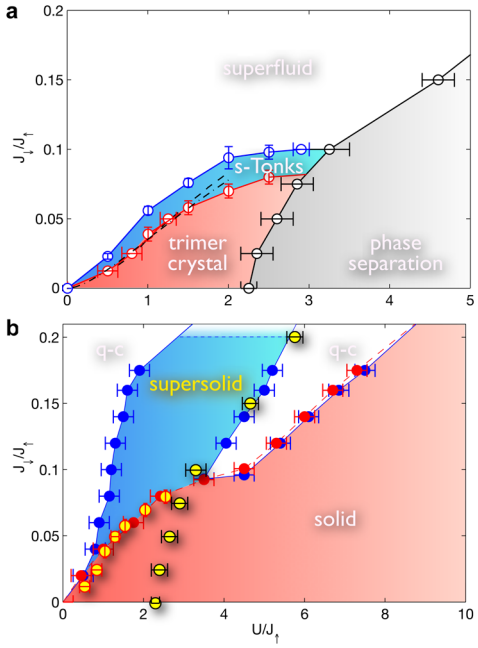

FIG. 2 (color online). Phase diagrams in and out of equilibrium. (a) Equilibrium phase diagram (empty circles). The dash-dotted line represents the points where the hopping of the ↓ bosons, $J_\downarrow$, overcomes the energy gap to crystal dislocations, giving rise to the solid–super-Tonks (s-Tonks) transition. The dashed line marks the points where a single-trimer wave function spreads over 2.8 sites. (b) Out-of-equilibrium phase diagram. An extended supersolid phase exists in the transient state attained after the quantum quench. Blue symbols (solid lines) delimit the boundaries of the solid phase, red symbols (dashed lines) mark the lower boundary for the quasicondensed (q-c) phase. The overlap of both phases (blue shaded region) is identified as the supersolid phase. The yellow (light) filled symbols correspond to equilibrium data points. The lower boundary of the superfluid–super-Tonks region of the equilibrium phase diagram is seen to coincide with the lower boundary of the supersolid region out of equilibrium.

For the considered filling it can be shown via exact diagonalization that, at sufficiently low attraction $U/J_\uparrow \leq 2.3$, the ground state realizes a crystal of *trimers* formed by two ↓ bosons "glued" together by an ↑ boson in an atomic analogue of a covalent bond [see Fig. 1(a) for a scheme of the spatial arrangement]. The trimer crystal is protected by a finite energy gap against dislocations of the ↓ bosons, and hence it is expected to survive the presence of a small hopping $J_\downarrow$. We have tested this hypothesis with extensive quantum Monte Carlo simulations based on the canonical stochastic series expansion algorithm [11,12]. Simulations have been performed on chains of size $L = 30, \ldots, 120$ with periodic boundary conditions, at an inverse temperature $\beta J_\downarrow = 2L/3$ ensuring that the obtained data describe the zero-temperature behavior for both atomic species.

Figure 2(a) shows the resulting ground-state phase diagram, which features indeed an extended trimer-crystal phase. For $U/J_\uparrow \geq 2.3$, and over a large region of $J_\downarrow/J_\uparrow$ ratios, the ground state shows instead the progressive merger of the trimers into hexamers, dodecamers, and finally into a fully collapsed phase with phase separation of the system into particle-rich and particle-free regions.

For $U/J_\uparrow \lesssim 2.3$, increasing the $J_\downarrow/J_\uparrow$ ratio allows one to continuously tune the zero-point quantum fluctuations of the ↓ atoms in the trimer crystal and to increase the effective size of the trimers, whose wave functions start to overlap. We find that, when trimers spread over a critical size of ≈ 2.8 lattice sites, they start exchanging atoms and the quantum melting of the crystal is realized. The melting point is also consistent with the point at which the hopping $J_\downarrow$ overcomes the energy gap to dislocations [dash-dotted line in Fig. 2(a)]. The resulting phase after quantum melting is a one-dimensional superfluid for both atomic species: in this phase quasicondensation appears, in the form of power-law decaying phase correlations $\langle b^\dagger_{i,\sigma} b_{j,\sigma} \rangle \propto |r_i - r_j|^{-\alpha_\sigma}$, which is the strongest form of off-diagonal correlations possible in interacting one-dimensional quantum models [13]. Yet in the superfluid phase strong power-law density correlations survive, $\langle n_{i,\sigma} n_{j,\sigma} \rangle \propto \cos[q_{\text{tr}}(r_i - r_j)]|r_i - r_j|^{-\beta_\sigma}$, exhibiting oscillations at the trimer-crystal wave vector $q_{\text{tr}} = 2\pi/3$. Such correlations stand as remnants of the solid phase, and in a narrow parameter region they even lead to a *divergent* peak in the density structure factor, $S_\sigma(q_{\text{tr}}) \propto L^{\beta_\sigma}$ with $0 < \beta_\sigma < 1$, where

$$S_\sigma(q) = \frac{1}{L} \sum_{ij} e^{iq(r_i - r_j)} \langle n_{i,\sigma} n_{j,\sigma} \rangle. \quad (2)$$

This phase, termed "super-Tonks" phase in the literature on one-dimensional quantum systems [14], is a form of quasisupersolid, in which one-dimensional superfluidity coexists with quasisolid order. (Notice that true solidity corresponds to $\beta_\sigma = 1$.)

The strong competition between solid order and superfluidity in the ground-state properties of this model suggests the intriguing possibility that true supersolidity might

appear by perturbing the system out of the above equilibrium state. In particular, we investigate the Hamiltonian evolution of the system after its state is prepared out of equilibrium in a perfect trimer crystal. The initial state is a simple factorized state of perfect trimers [see Fig. 1(a)]: $|\Psi_0\rangle = \otimes_{n=1}^{L/3} |\Phi_{\rm tr}^{(3n-1)}\rangle$, where the trimer wave function reads $|\Phi_{\rm tr}^{(i)}\rangle = \frac{1}{\sqrt{2}} b_{i\downarrow}^\dagger b_{i+1\downarrow}^\dagger (b_{i\uparrow}^\dagger + b_{i+1\uparrow}^\dagger)|{\rm vac}\rangle$. This state can be realized with the current technology of optical superlattices [15], by applying a strong second standing wave component $V_{x_2}\cos^2[(k/3)x + \pi/2]$ to the primary wave $V_{x_1}\cos^2(kx)$, creating the optical lattice along the x direction of the chains. This superlattice potential has the structure of a succession of double wells separated by an intermediate, high-energy site. Hence tunneling out of the double wells is strongly suppressed, stabilizing the factorized state $|\Psi_0\rangle$. After preparation of the system in the initial state, the second component of the superlattice potential is suddenly switched off ($V_{x_2} \to 0$) and the state is evolved with the Hamiltonian corresponding to different parameter sets ($U/J_\uparrow$, $J_\downarrow/J_\uparrow$). The successive time evolution over a short time interval $[0, \tau]$ with $\tau = 3\hbar/J_\downarrow$ is computed using the matrix-product-states algorithm on a one-dimensional lattice with up to 28 sites and open boundary conditions [16]. A bond dimension $D = 500$ ensures that the weight of the discarded Hilbert space is $<10^{-3}$. The evolution time step $dt = 5 \times 10^{-3}\hbar/J_\uparrow$ is chosen so as to make the Trotter error smaller than 10^{-3}. We characterize the evolved state by averaging the most significant observables over the last portion of the time evolution $\tau/3$.

We find three fundamentally different evolved states, whose extent in parameter space is shown on the nonequilibrium phase diagram of Fig. 2(b). First, we observe a superfluid phase, in which the initial crystal structure is completely melted by the Hamiltonian evolution and where coherence builds up leading to quasicondensation out of equilibrium, namely, to the appearance of a (sublinearly) diverging peak in the momentum distribution $\langle n_k^\sigma\rangle = \frac{1}{L}\sum_{ij} e^{ik(r_i - r_j)}\langle b_{i,\sigma}^\dagger b_{j,\sigma}\rangle$ at zero quasimomentum, $\langle n_{k=0}^\sigma\rangle \propto L^{\alpha_\sigma}$ with $0 < \alpha_\sigma < 1$. Despite the short time evolution, quasicondensation of the slow $\downarrow$ bosons is probably assisted by their interaction with the faster $\uparrow$ bosons, and is observed to occur for all system sizes considered. Second, we find a solid phase, in which the long-range crystalline phase of the initial state is preserved, as shown by the structure factor which has a linearly diverging peak at the trimer-crystal wave vector $S(q_{\rm tr}) \propto L$. Third, an extended supersolid phase emerges, with perfect coexistence of the two above forms of order for both atomic species. This is demonstrated in Figs. 3(a) and 3(b) via the finite-size scaling of the peaks in the momentum distribution and in the density structure factor. In this phase, which has no equilibrium counterpart, the Hamiltonian evolution leads to the delocalization of a significant fraction of $\uparrow$ and $\downarrow$ bosons over the entire system size. Consequently quasi-long-range coherence builds up and the momentum distribution, which is completely flat in the initial localized trimer-crystal state, acquires a pronounced peak at zero quasimomentum $k = 0$, as shown in Fig. 1(b). Yet the quasicondensation order parameter $\chi_i^{(0)}$, namely, the natural orbital of the one-body density matrix (OBDM) $\langle b_{i,\sigma}^\dagger b_{j,\sigma}\rangle$ corresponding to the largest eigenvalue and hosting the condensed particles, is spatially modulated [cf. Fig. 3(c)], revealing the persistence of solid order in the quasicondensate. In addition, solidity can be confirmed by direct inspection of the real-space density $\langle n_{i\sigma}\rangle$ [cf. inset of Fig. 1(b)]. Going from the boundaries towards the center, the density profiles of both species are modulated by the crystal structure, and the modulation amplitudes saturate at constants which turn out to be independent of the system size.

To gain further insight into the mechanism underlying the stabilization of a commensurate two-species supersolid via out-of-equilibrium time evolution, we finally compare the equilibrium phase diagram with the nonequilibrium one. Figure 2(b) shows that the superfluid-solid and superfluid–phase-separation boundaries at equilibrium overlap with the threshold of formation of the supersolid

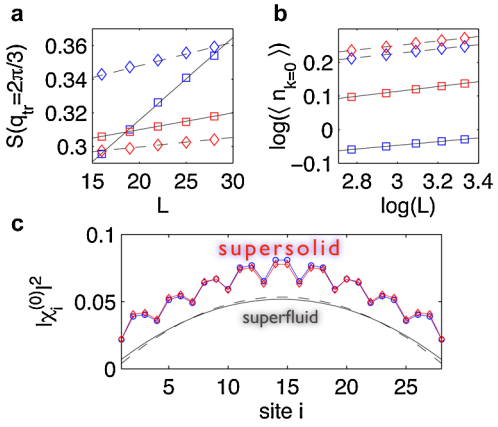

FIG. 3 (color online). Coexistence of solid order and quasicondensation in the supersolid phase. (a) The structure factor peak $S(q_{\rm tr} = 2\pi/3)$ scales linearly with system size L, demonstrating solid order for both bosonic species. (b) The density peak in momentum space $\langle n_{k=0}^\downarrow\rangle$ is plotted versus L on a log-log scale, showing algebraic scaling and thus quasicondensation. Boxes (diamonds) stand for particle species $\downarrow$ ($\uparrow$), respectively. The data represented by dark (blue) boxes in (a) are offset by -0.2 for better visibility. Parameters: $J_\downarrow/J_\uparrow = 0.1$, $U/J_\uparrow = 3.0$ [dark (blue) symbols] and $J_\downarrow/J_\uparrow = 0.15$, $U/J_\uparrow = 2.5$ [light (red) symbols]. (c) Square modulus of the natural orbital $\chi_i^{(0)}$ corresponding to the largest eigenvalue of the OBDM, calculated at final time τ. In the supersolid regime [dark (blue) symbols and light (red) symbols for $\downarrow$ and $\uparrow$ bosons], the natural orbital shows the characteristic crystalline order. This pattern is washed out in the purely quasicondensed regime (dashed curves and solid curves for $\downarrow$ and $\uparrow$). The supersolid data are offset by $+0.02$ for the sake of visibility. Parameters: $J_\downarrow/J_\uparrow = 0.1$ (supersolid), $J_\downarrow/J_\uparrow = 0.8$ (quasicondensed), $U/J_\uparrow = 3.0$, $N_\downarrow = 18$, $N_\uparrow = 9$, $L = 28$.

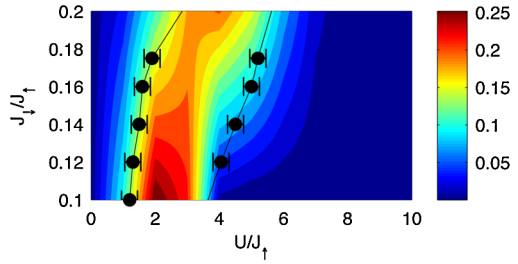

FIG. 4 (color online). Overlap of the equilibrium ground state with the initial trimer-crystal state. The overlap $|c_0|^2$ (contour plot) agrees well with the boundaries of the nonequilibrium supersolid phase [black symbols, cf. Fig. 2(b)]. This suggests a superfluid ground state as a necessary condition for supersolidity to dynamically set in. The overlap $|c_0|^2$ has been calculated via exact diagonalization on a $L = 10$ chain containing three trimers.

out of equilibrium upon increasing $J_\downarrow/J_\uparrow$. This means that a quantum quench of the system Hamiltonian to the parameter range corresponding to a superfluid equilibrium ground state is a necessary condition for supersolidity to dynamically set in.

The key to the dynamical emergence of a quasicondensate fraction in the supersolid phase is that the initial trimer-crystal state $|\Psi_0\rangle$ has a significant overlap with the superfluid ground state of the final Hamiltonian after the quantum quench. As shown in Fig. 4 for a small cluster with $L = 10$ sites, the ground-state overlap $|c_0|^2$ remains sizable over an extended parameter range. This is intimately connected with the strong density-density correlations present in the equilibrium superfluid phase, as shown, e.g., by the appearance of a region with super-Tonks behavior. The excellent agreement between the region featuring supersolidity and the region with most pronounced overlap $|c_0|^2$ suggests the following mechanism: the Hamiltonian evolution following the quantum quench dynamically selects the ground-state component as the one giving the dominant contribution to (quasi)long-range coherence. In essence, while the quantum melting phase transition occurring at equilibrium leads to a dichotomy between solid and superfluid order, the out-of-equilibrium preparation can coherently admix the excited crystalline state(s) with the superfluid ground state without disrupting their respective forms of order [17]. It is tempting to think that a similar preparation scheme of supersolid states can work in other systems displaying solid-superfluid phase boundaries at equilibrium.

The supersolid transient state is an exquisitely nonequilibrium state, because no order can survive at finite temperature in 1D systems with short-range interactions. An intriguing question arises then: in the long-time limit $\tau \gg 3\hbar/J_\downarrow$ (which is only accessible numerically on very small system sizes) does supersolidity survive or is long-range order ultimately destroyed by thermalization? Recent numerical studies point towards the failure of other strongly correlated one-dimensional quantum systems to thermalize [18]. We have considered the asymptotic time limit using exact diagonalization for a small system [17]. These exact results suggest that supersolidity persists and the system does not converge to an equilibrium thermal state (in fact even thermalization in the microcanonical ensemble, proposed in Ref. [19], does not seem to occur in our system). Whether the absence of thermalization survives when taking the thermodynamic limit remains an open question, whose answer at the moment can only rely on experiments.

The observation of the supersolid state prepared via the dynamical scheme proposed in this Letter is directly accessible to several setups in current optical-lattice experiments; see [17] for details. A particularly intriguing feature is that the emergence of the supersolid occurs after a very short time (1–10 ms), eluding therefore possible decoherence effects.

We thank J. J. Garcia-Ripoll, M. Roncaglia, and R. Schmied for helpful discussions. This work is supported by the European Union through the SCALA integrated project.

[1] A. J. Leggett, Phys. Rev. Lett. **25**, 1543 (1970); G. V. Chester, Phys. Rev. A **2**, 256 (1970).
[2] E. Kim and M. H. W. Chan, Nature (London) **427**, 225 (2004); J. Day and J. Beamish, Nature (London) **450**, 853 (2007).
[3] N. Profok'ev, Adv. Phys. **56**, 381 (2007).
[4] M. H. W. Chan, Science **319**, 1207 (2008).
[5] I. Bloch, J. Dalibard, and W. Zwerger, Rev. Mod. Phys. **80**, 885 (2008).
[6] D. Jaksch, Nature (London) **442**, 147 (2006).
[7] I. Titvinidze, M. Snoek, and W. Hofstetter, Phys. Rev. Lett. **100**, 100401 (2008); F. Hebert, G. G. Batrouni, X. Roy, and V. G. Rousseau, Phys. Rev. B **78**, 184505 (2008).
[8] D. Jaksch *et al.*, Phys. Rev. Lett. **81**, 3108 (1998).
[9] B. Paredes *et al.*, Nature (London) **429**, 277 (2004).
[10] L. M. Falicov and J. C. Kimball, Phys. Rev. Lett. **22**, 997 (1969).
[11] A. W. Sandvik, Phys. Rev. B **59**, R14 157 (1999).
[12] T. Roscilde, Phys. Rev. A **77**, 063605 (2008).
[13] T. Giamarchi, *Quantum Physics in One Dimension* (Clarendon, Oxford 2003).
[14] G. E. Astrakharchik *et al.*, Phys. Rev. Lett. **95**, 190407 (2005).
[15] S. Fölling *et al.*, Nature (London) **448**, 1029 (2007).
[16] G. Vidal, Phys. Rev. Lett. **93**, 040502 (2004); J. J. Garcia-Ripoll, New J. Phys. **8**, 305 (2006).
[17] See EPAPS Document No. E-PRLTAO-103-006928 for exact calculations of the evolved trimer state and experimental considerations. For more information on EPAPS, see http://www.aip.org/pubservs/epaps.html.
[18] C. Kollath, A. Läuchli, and E. Altman, Phys. Rev. Lett. **98**, 180601 (2007); S. R. Manmana *et al.*, Phys. Rev. Lett. **98**, 210405 (2007).
[19] M. Rigol, V. Dunjko, and M. Olshanii, Nature (London) **452**, 854 (2008).